Intensity fluctuations of a recorded signal in visual laser navigation aids

G.A. Kaloshin and V.V. Nosov

Institute of Atmospheric Optics,
Siberian Branch of the Russian Academy of Sciences, Tomsk

Received July 22, 2002

We study joint effect of specific features of the laser beam scanning and intensity fluctuations due to atmospheric turbulence on a signal recorded on horizontal paths with the visual laser navigation aids (LVNA). An experimental setup based on an ILD-2 laser dosimeter is considered as applied to measurement of the shape and duration of laser beacon signals. The estimated standard deviation of the intensity fluctuations at a receiver under different propagation conditions and for paths of up to ten kilometers long is compared with measured signal fluctuations being caused by scanning system. The range of signal variation under the joint effect of both factors is estimated, as well as the corresponding brightness fluctuations at visual observation. It is shown that the allowance for the joint effect of atmospheric turbulence and scanning is important both for obtaining quantitative data on fluctuations of the signal recorded and for developing engineering solutions to reduce this effect.

Operation of the visual laser navigation aids (LVNA) assumes formation of orientation sectors by scanning a laser beam to achieve the maximum level of signal. The horizontal and vertical scanning frequencies in this case differ by hundreds times.[1,2] As a consequence, the recorded signal (flash) consists of a pulse burst, whose envelope copies the intensity distribution of a laser beam and the number of pulses in the burst changes with time. Correspondingly, the energy of flashes recorded with a stationary receiver fluctuates. Along with this, the laser beam intensity fluctuates in the turbulent atmosphere on the inhomogeneities of the air refractive index. Therefore, it is interesting to estimate the joint effect of these phenomena on the recorded signal.

Intensity fluctuations of a signal due to scanning

The effective illumination E_{eff} at visual observation of the flashing signal lights is described by the empirical Blondel—Ray equation, which is good for rectangular shaped flashes.[3] At present, owing to the advent of various light sources, including pulsed ones, E_{eff} determined in the empirical way is described by the Schmidt–Clausen equation: $E_{\text{eff}} = E_{\max}\,\tau_{\text{f}}/(a_{\text{BR}}F^{-1} + \tau_{\text{f}})$ (Ref. 4). Here $E_{\max}$ is the maximum value of illumination within a single flash; τ_{f} is the flash duration; a_{BR} is the Blondel—Ray constant equal to 0.3–0.1 s depending on the source parameters and the observation conditions; F is the coefficient (shape factor) numerically equal to the ratio of the areas under the flash curve and under the rectangular flash with the same duration and the maximum illumination value. In particular, for the case of recording the LVNA flashes, whose intensity distribution is described by a Gaussian curve, $F = 0.584$. The parameter F is introduced to replace the available flash profile with the rectangular one having the same duration and the maximum illumination, but with the following correction through the shape factor.

To estimate quantitatively intensity fluctuations of a signal due to scanning, a laser beam control device of the Mars-1 leading beacon was used.[2] Note that in this paper we do not consider causes of signal fluctuations due to scanning. Detailed consideration of these causes is a subject of a separate study. Flashes were recorded with an ILD-2 laser dosimeter, which measured the energy and energy density of single radiation flashes, flash duration τ_{f} from 10^{-6} to 10^{-2} s, and the maximum value of the flash energy with the error no larger than 12%. For the most characteristic angles and time characteristics of scanning equal to $f_{\text{hor}} = 1$ Hz, $\gamma_{\text{hor}} = 3°$ and $\gamma_{\text{vert}} = 1.5°$, the normalized standard deviation of the flash energy density measured was $\sigma_I^{\text{scan}} = 0.17$.

Visual perception depends on retina illumination, which is proportional to the brightness of an observed object. However, the relation between the retina illumination and the sensation is rather complicated and nonlinear.[5] According to the Weber—Fechner law, the sensation of luminosity variation from B to B_1 at visual detection of light is proportional to the log change of brightness from L_1 to L or, analytically,

$$B - B_1 = \frac{1}{\varepsilon} \ln \frac{L}{L_1},$$

0235-6880/02/12 997-05 $02.00

where ε is the threshold contrast equal to 0.02 in the rather wide brightness range. Assuming that the luminosity is equal to unity for the threshold brightness, we obtain

$$B = \frac{1}{\varepsilon} \ln \frac{L}{L_1} + 1.$$

Then, the experimentally measured characteristic luminosity change B_{scan} due to scanning is equal to 8.85, that is, the value equal to 8.85 threshold values of the brightness difference.

Effect of atmospheric turbulence

As the laser beam propagates through the atmosphere, the light energy in the beam cross section redistributes considerably. Wave front distortions introduced by turbulent fluctuations of the air refractive index lead to intensity fluctuations of the light wave. The atmospheric turbulence affects also the beam geometry, causing turbulent broadening and random shifts of the beam as a whole.

Let us estimate the effect of atmospheric turbulence on the signal energy and frequency spectrum. In the context of energy of the recorded signal, the random spatial intensity modulation is characterized by the relative root-mean-square (rms) deviation of the intensity fluctuations σ_I, whose square is the normalized variance of intensity fluctuations

$$\sigma_I^2 = (\langle I^2 \rangle - \langle I \rangle^2) / \langle I \rangle^2,$$

where I is the random radiation intensity; σ_I is sometimes referred to as the scintillation index.

It is of practical interest for LVNA to know the visually resolved low-frequency part of the temporal frequency spectrum of the intensity fluctuations. Since the frequency spectrum characterizes the frequency distribution of the energy of intensity fluctuations, the parameter

$$P(f)/P_0 = \int_0^f \mathrm{d}f' \; W_I(f') / \int_0^\infty \mathrm{d}f' \; W_I(f')$$

corresponds to the fraction of energy falling within the frequency range $0 \le f' \le f$ in the total energy of fluctuations. Here $W_I(f')$ is the frequency spectrum of the intensity fluctuations (Fourier transform of the non-normalized time correlation function); P_0 is the total energy of fluctuations (spectral interval over all frequencies), $P_0 = \langle I^2 \rangle - \langle I \rangle^2 = P(\infty)$; f is some cutoff frequency; $0 \le P(f)/P_0 \le 1$.

As known,[3] vision has some persistence, which mostly depends on the background brightness B_{b}. The persistence of vision is characterized by the persistence time determined as $\theta = 0.13–0.08 \tanh(\log B_{\text{b}} + 1)$. Along with this, the persistence of vision is characterized by the critical flicker fusion frequency f_{cr}, at which an observer stops to perceive a decrease or an increase in brightness. For $\theta = 0.05$ s $f_{\text{cr}} \approx 25$ Hz. In particular, if $f = f_{\text{cr}}$, then $P(f_{\text{cr}})/P_0$ characterizes the relative energy of fluctuations resolved by eye. It is clear that at $P(f_{\text{cr}})/P_0 \ll 1$ intensity fluctuations occur mostly at the frequencies exceeding the critical frequency f_{cr} ($f_{\text{cr}} \le f < \infty$), and intensity variations in time in this case are hardly resolvable by eye. In the opposite case, when $P(f_{\text{cr}})/P_0 \to 1$, almost entire energy of fluctuations is concentrated in the interval $0 \le f \le f_{\text{cr}}$, and the time variations are clearly seen.

Estimate now σ_I and $P(f_{\text{cr}})/P_0$ for typical conditions on horizontal LVNA–observer paths. For the conditions of navigation with LVNA, the mean height of an optical path above the sea surface h_T usually varies from 10 to 20 m. For such a height, the line-of-sight conditions take place at the paths with the length l up to 20 km. The mean height of the path in calculations is assumed equal to 15 m, and its length is thought variable within the above range. The typical parameters of laser sources used in LVNA range as

$$0.5\ \mu\text{m} \le \lambda \le 0.7\ \mu\text{m}; \quad 4\ \text{mm} \le 2a \le 10\ \text{mm};$$

$$4\ \text{arc min} \le \varphi_0 \le 10\ \text{arc min},$$

where λ is the radiation wavelength; a is the radius of the emitting aperture; φ_0 is the total angle of the initial beam divergence.

For these source and path parameters, the Fresnel number of the emitting aperture is

$$\Omega = ka^2/l,$$

where $k = 2\pi/\lambda$ is the wave number satisfying the inequality $\Omega \ll 1$. This means[6–9] that LVNA operates in the mode of a quasi-spherical wave, which is characterized by small Fresnel numbers and the laser beam divergence angles φ_0 typical of LVNA.

According to Refs. 6 to 9, the normalized rms deviation of the intensity fluctuations of a spherical wave σ_I is described by the following asymptotic equations:

$$\begin{aligned} \sigma_I &= 0.63\ \beta_0 \text{ at } \beta_0 \ll 1, \\ \sigma_I &= 1 + 1.4\ \beta_0^{-4/5} \text{ at } \beta_0 \gg 1; \\ \beta_0^2 &= 1.23\ C_n^2(h_T)\ k^{7/6}\ l^{11/6}, \end{aligned} \qquad (1)$$

where $C_n^2(h_T)$ is the structure characteristic of fluctuations of the air refractive index under continental, coastal, and sea conditions, respectively, as measured at the height h_T of the beam propagation. The parameter β_0 in Eqs. (1) characterizes the combined effect of atmospheric turbulence on the propagation of optical radiation. The intervals $\beta_0 \le 1$ and $\beta_0 \ge 1$ specify the regions of weak and strong intensity fluctuations, respectively. In the intermediate region where $\beta_0 \approx 1$, the value of σ_I can be estimated using data from Ref. 9.

To calculate $P(f)/P_0$, let us use the frequency spectra of a quasi-spherical wave in accordance with

Refs. 6–9. Normalized frequency spectra usually turn out to have significantly different frequencies. Therefore, the integral of the spectrum (value of $P(f)/P_0$) is determined, first, by the position of the maximum of the normalized spectrum on the frequency axis. The dependence on the spectral density (at variation of the path, source, and atmospheric parameters) is significantly less pronounced and it can be neglected in calculations that do not require very high accuracy.

The position of maximum of the normalized spectrum is determined by the corresponding characteristic frequency of time fluctuations. The characteristic frequencies in the regions of weak and strong fluctuations are described by different equations.[6–9] Let us join these equations and generalize the resulting equation for the case of a fluctuating wind based on data from Ref. 8. As a result, the characteristic frequency of time fluctuations f_0 can be presented as follows:

$$f_0 = (1 + 3.12\,\beta_0^{6/5})\sqrt{(v_+^2 + \sigma_+^2)/(2\pi\lambda l)}, \qquad (2)$$

where v_+ is the absolute value of the wind velocity component normal to the optical path ($v_+ = |\mathbf{v}_+|$); σ_+ is the absolute value of the vector of random fluctuations of the cross wind component (vector of deviations of the cross wind component from its mean value) ($\sigma_+ = |\boldsymbol{\sigma}_+|$). In the particular cases of weak and strong fluctuations, the equations for the characteristic frequencies corresponding to them follow from Eq. (2) (Refs. 6–9). In this case, the frequency f_0 is determined by the velocity of wind-driven transport of turbulent inhomogeneities across the beam along the radius of the first Fresnel zone (weak fluctuations) or along the coherence length of the field of a spherical wave (strong fluctuations).

Calculation of $P(f)/P_0$ performed with the use of experimental data for the frequency spectrum of a quasi-spherical wave[6] shows that radiation intensity fluctuations occur mostly at the frequencies that do not exceed the frequency $f_n = nf_0$, whose value corresponds to the sum of several characteristic frequencies of the intensity fluctuations f_0 ($0 \le f \le nf_0$; $P(f)/P_0 = 0.65$ at $n = 2$; $P(f)/P_0 = 0.81$ at $n = 3$; $P(f)/P_0 = 0.91$ at $n = 4$).

To predict the values of σ_I and $P(f_{cr})/P_0$ for typical conditions of continental, coastal, and sea LVNA–observer paths, it is necessary to calculate the complex parameter β_0 in Eqs. (1) and (2) for these conditions. For this purpose, we should specify typical values of the structure characteristic $C_n^2(h_T)$ at the path height h_T.

Let us use a phenomenological model of the altitude profile of the structure characteristic[6–9] constructed by means of generalization of the experimental data. The values of $C_n^2(h)$ observed in the surface layer at the height $h = 2.5$ m are divided into four groups in this model:

$$\begin{aligned}
&1)\ C_n^2(h) \ge C_{n\,1}^2 = 5 \cdot 10^{-15}\ \text{cm}^{-2/3},\\
&2)\ C_{n\,1}^2 > C_n^2(h) \ge C_{n\,2}^2 = 3 \cdot 10^{-16}\ \text{cm}^{-2/3},\\
&3)\ C_{n\,2}^2 > C_n^2(h) \ge C_{n\,3}^2 = 2 \cdot 10^{-17}\ \text{cm}^{-2/3},\\
&4)\ C_{n\,3}^2 > C_n^2(h).
\end{aligned} \qquad (3)$$

Each group of values in Eqs. (3) corresponds to the limiting dependences characteristic of the atmospheric surface layer. Based on data from Refs. 7 and 10 to 12, we can state that each group in Eqs. (3) is characteristic of different turbulent modes occurring in the atmosphere. These modes correspond to different atmospheric temperature stratifications established over vast territories. Consequently, each group of $C_n^2(h)$ values in Eqs. (3) can be considered as corresponding to some typical stable state of atmospheric turbulence. For the sake of brevity, each of such states (that is, each group in Eqs. (3)) can be represented by some typical selected value of $C_n^2(h)$.

Based on analysis of theoretical and experimental results of Refs. 7 and 10–12, we can show the most probable variability ranges of the surface $C_n^2(h)$ values (numbers of the groups in Eqs. (3)), which can occur depending on the latitude of an observation site, surface structure, season, time of a day, and the type of weather. It is clear that because of a wide variety of types of the surface and the weather and climate conditions characterizing that or other geographical region, this classification is conditional to a high extent. Nevertheless, it allows us to follow the dynamics of variations of the surface values of $C_n^2(h)$ in different weather-climate and geographical zones.

Tables 1 to 3 present the most probable numbers of the groups of the surface $C_n^2(h)$ values in Eqs. (3) depending on the latitude of an observation site and the surface type (Table 1), season, and time of a day (Table 2), as well as the weather type and the strength of wind (Table 3). When compiling these tables, we took (as the initial or standard conditions) the conditions, at which the value of $C_n^2(h)$ in mid-latitudes is maximum. These conditions correspond to a fine calm summer day at a dry open plain in mid-latitudes. Each table gives the deviations from the accepted initial conditions for the corresponding groups of parameters. To obtain the probable numbers of the groups of $C_n^2(h)$ values for arbitrary weather and climate conditions in different geographic zones, one should first find the probable number of the group in one of the Tables 1–3 (for example, in Table 1), then pass to the next table (for example, Table 2), and based on the dynamics of variation of the group numbers in this table (Table 2) correct the number of the group found from the previous table (Table 1). After obtaining the corrected group number, he/she should pass on to the next table (Table 3) and perform the next correction of the group number in a similar way.

Table 1. Most probable numbers of groups of the surface $C_n^2(h)$ values in Eqs. (3) depending on the latitude of the observation site and types of the surface (mean heights above the sea level: flat ground 0–200 m, highlands 200–600 m). Fine summer day, low wind

Latitude of observation site	Type of the surface			
	open flat land	flat billowy land	highland	sea
High	2	2–3	3–4	3–4
Middle	1	1–2	2–3	2
Low	1	1	2	1

Table 2. Most probable numbers of groups of the surface $C_n^2(h)$ values in Eqs. (3) depending on the season and time of day. Mid-latitudes, open flat land. Clear sky, weak wind

Season	Time of a day		
	daytime	morning, evening	night
Summer	1	1–2	2
Spring, fall	2	2–3	3
Winter	3–4	3–4	4

Table 3. Most probable numbers of groups of the surface $C_n^2(h)$ values in Eqs. (3) depending on the type of weather and the strength of wind. Mid-latitudes, open flat land. Summer, daytime

Type of weather	Strength of wind	
	Weak wind (up to 5 m/s)	Strong wind (above 5 m/s)
Fine	1	2–3
Cloudy (marked cloudiness, precipitation)	2	3

Since the lengths of the second and third ranges of the values in Eqs. (3) are almost the same on the log scale, it is natural to select the $C_n^2(h)$ values corresponding to the range centers as representatives of these ranges. For the first and fourth ranges in Eqs. (3), their representatives can be the $C_n^2(h)$ values spaced by the half-length of the second (or third) range from the range boundaries. Thus, for typical representatives of each of the ranges in Eqs. (3) we obtain the following values:

$$1)\ 2 \cdot 10^{-14}\ \text{cm}^{-2/3}, \quad 2)\ 1.2 \cdot 10^{-15}\ \text{cm}^{-2/3},$$
$$3)\ 8 \cdot 10^{-17}\ \text{cm}^{-2/3}, \quad 4)\ 5 \cdot 10^{-18}\ \text{cm}^{-2/3}. \qquad (4)$$

To transfer the values (4) to the beam height h_T, one should, using the model from Refs. 7 and 8, multiply the values (4) by $(h_T/h)^{-\alpha}$, where $\alpha = 4/3$, $2/3$, and 0, respectively, for the group 1, groups 2 and 3, and group 4 from Eqs. (3) and (4).

Figures 1 and 2 depicts the plots of the functions $P(f_{cr})/P_0$ and σ_I depending on the path length for the values (4) of the structure characteristic $C_n^2(h_T)$ at the height $h_T = 15$ m. The plots have been drawn for a quasi-spherical wave at $\lambda = 0.63$ μm.

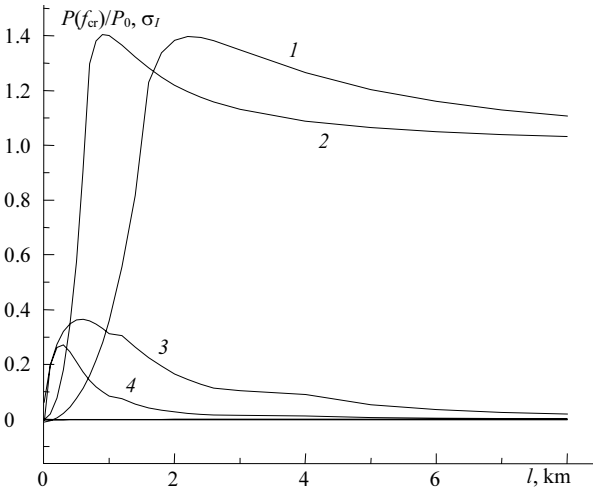

Fig. 1. Dependences of $P(f_{cr})/P_0$ and σ_I for typical $C_n^2(h_T)$ values of the first and second groups in Eqs. (3) and (4) on the path length l: curves *1* and *2* correspond to σ_I; curves *3* and *4* are for $P(f_{cr})/P_0$; curves *2* and *4* are for the first group, and curves *1* and *3* are for the second group of values of the structure characteristic in Eqs. (3) and (4); for curves *3* and *4* $\sqrt{v_+^2 + \sigma_+^2} = 1$ m/s, $f_{cr} = 25$ Hz.

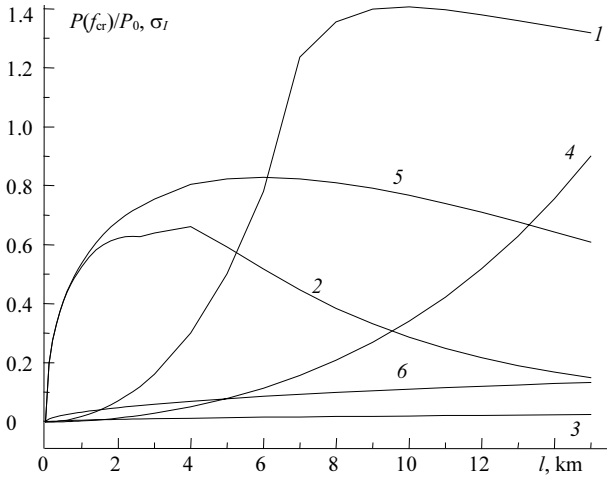

Fig. 2. Dependences of $P(f_{cr})/P_0$ and σ_I for typical $C_n^2(h_T)$ values of the third and fourth groups in Eqs. (3) and (4) on the path length l: curves *1* and *4* correspond to σ_I; curves *2*, *3*, *5*, and *6* are for $P(f_{cr})/P_0$; curves *1*, *2*, and *3* are for the third group, and curves *4*, *5*, and *6* are for the fourth group of values of the structure characteristic in Eqs. (3) and (4). For curves *2* and *5* $\sqrt{v_+^2 + \sigma_+^2} = 1$ m/s and for curves *3* and *6* $\sqrt{v_+^2 + \sigma_+^2} = 5$ m/s, $f_{cr} = 25$ Hz.

Discussion

As shown in Figs. 1 and 2, as the turbulence intensity on a path decreases (at transition from the first group of values in Eqs. (3) and (4) to the fourth one), σ_I decreases on the average, and the fraction of fluctuation energy falling in the frequency range $0 \le f \le f_{cr}$ and characterized by the function $P(f_{cr})/P_0$ increases. This means that for the third and fourth

groups at a weak cross wind the time variations of the intensity (luminosity) of the recorded LVNA signals are well resolved by eye.

Note that, according to the definition (2) of the characteristic frequency of time intensity fluctuations f_0, the weak cross wind mode takes place either at almost calm weather ($v_+ \le 1$–3 m/s, $\sigma_+ \approx 0$) or at the wind of arbitrary strength, whose velocity vector is directed parallel to the optical path ($v_+ \approx 0$, $\sigma_+ \le 1$–3 m/s).

For the first and the second groups, the time fluctuations of the source intensity are almost unresolved by eye (or weakly resolved), but random intensity variations for these groups are significant. For long paths (more than 2 km long) $\sigma_I \ge 1$ that means 100% intensity modulation. For such modulation, even a small energy fraction of fluctuations from the frequency range $0 \le f \le f_{cr}$ resolved by eye is sufficient.

Comparing the rms deviations of signal fluctuations arising due to scanning σ_I^{scan} ($\sigma_I^{scan} = 0.17$) and due to atmospheric turbulence σ_I, we can see from Figs. 1 and 2 that they coincide ($\sigma_I^{scan} = \sigma_I$) at $l = 0.3$, 0.74, 3.1, 7.1 km and $\sigma_I^{scan} = \sigma_I/2$ at $l = 0.4$, 0.96, 4.2, 9.95 km, respectively, for the first, second, third, and fourth groups of $C_n^2(h)$ values in Eqs. (3).

It follows from Tables 1–3 that the following groups of $C_n^2(h)$ values in Eqs. (3) almost never occur over sea: the first group in the mid-latitudes and the first and second groups in high latitudes. Consequently, the first and second groups of $C_n^2(h)$ are unlikely. Therefore, the contribution of fluctuations due to scanning to the total value of signal fluctuations turn out to be significant (at the distances up to 10 km) for large number of geographical zones under various weather and climate conditions.

If, for example, we take $\sigma_I = 0.4$ and $P(f)/P_0 = 0.85$ obtained for $l = 4$ and 10 km and $C_n^2(h)$ for the third and fourth groups as mean values, then the visual perception of luminosity variation will be $B_{turb} \approx 25.5$.

Comparison of B_{turb} and B_{scan} shows that B_{scan} has a considerable value and its contribution to the total value $B = B_{turb} + B_{scan}$ is significant. Taking into account that B_{scan} does not change at variation of the distance l, its contribution at small l will be comparable with or even exceeding B_{turb}.

Besides, luminosity variation due to scanning and due to the atmospheric turbulence has different frequency ranges. If in the first case it is ≈ 1 Hz, then in the second case the frequency of intensity fluctuations ranges from a few hertzs to several hundreds of hertzs. As was already mentioned, the persistence of vision is characterized by the critical flicker fusion frequency f_{cr}, at which an observer stops to see decrease or increase of brightness. For θ equal to 0.05 s $f_{cr} \approx 25$ Hz. This means that the contribution of B_{scan} to B is even more significant, because it is fully resolved by eye, while for B_{turb} it is visible only up to 20–25 Hz. Our measurements show[13] that the major contribution to the spectral distribution of the signal power is due to the frequencies higher than 20 Hz.

Consequently, B_{scan} should be reduced to a maximum possible degree in spite of some technical difficulties and expenses, keeping in mind that B_{turb} is caused by the atmospheric turbulence, which is unavoidable in principle.

It should be noted that the value of B_{turb} can be decreased if one increases the receiver's aperture at observation, for example, through binoculars.

References

1. V.E. Zuev, V.I. Peresypkin, G.A. Kaloshin, V.Ya. Fadeev, and R.S. Fedorov, *Laser Navigation Devices* (Nauka, Novosibirsk, 1985), 128 pp.
2. G.A. Kaloshin, in: *Materials of Scientific and Technical Seminar on High Dual-Purpose Technologies and Mechanisms of Their Realization on Military Enterprises* (Tomsk State University Publishing House, Tomsk, 1999), pp. 59–62.
3. A.V. Luizov, *Eye and Light* (Energoatom, Leningrad, 1983), 144 pp.
4. Cordell and J.G. Holmes, IALA Bull. **2**, 30–36 (1985).
5. V.V. Meshkov and A.B. Matveev, *Principles of Lighting Engineering.* Part 2. *Physiological Optics and Calorimetry* (Energoatomizdat, Moscow, 1989), 432 pp.
6. V.E. Zuev, V.A. Banakh, and V.V. Pokasov, *Optics of the Turbulent Atmosphere*. Series *Current Problems of Atmospheric Optics* (Gidrometeoizdat, Leningrad, 1988), 272 pp.
7. A.S. Gurvich, A.I. Kon, V.L. Mironov, and S.S. Khmelevtsov, *Laser Radiation in the Turbulent Atmosphere* (Nauka, Moscow, 1976), 277 pp.
8. V.L. Mironov, *Laser Beam Propagation through the Turbulent Atmosphere* (Nauka, Novosibirsk, 1981), 247 pp.
9. V.P. Aksenov, A.V. Alekseev, V.A. Banakh, V.M. Buldakov, V.V. Veretennikov, A.F. Zhukov, M.V. Kabanov, G.M. Krekov, Yu.S. Makushkin, V.L. Mironov, A.A. Mitsel', N.F. Nelyubin, V.V. Nosov, Yu.N. Ponomarev, Yu.A. Pkhalagov, and K.M. Firsov, *Effect of the Atmosphere on Laser Radiation Propagation*, ed. by V.E. Zuev and V.V. Nosov, Vol. II, (TA SB AS USSR Publishing House, Tomsk, 1987), 247 pp.
10. A.S. Monin and A.M. Yaglom, *Statistical Fluid Mechanics: Mechanics of Turbulence*, Vol. 1, (The MIT Press, Cambridge, Massachusetts, 1971), 769 pp.
11. S.S. Zilitinkevich, *Dynamics of Atmospheric Boundary Layer* (Gidrometeoizdat, Leningrad, 1970).
12. P.N. Tverskoi, *Course of Meteorology (Atmospheric Physics)* (Gidrometeoizdat, Leningrad, 1962), 700 pp.
13. B.V. Goryachev and G.A. Kaloshin, in: *Scattering and Refraction of Optical Waves in the Atmosphere* (IAO SB AS USSR, Tomsk, 1976), pp. 63–68.